



## Physical-Chemical Properties of the Support Immobead 150 Before and After the Immobilization Process of Lipase

Carla R. Matte,<sup>a</sup> Carolina Bordinhão,<sup>a</sup> Jakeline K. Poppe,<sup>a</sup> Edilson V. Benvenuti,<sup>b</sup>  
Tania M. H. Costa,<sup>b</sup> Rafael C. Rodrigues,<sup>a</sup> Plinho F. Hertz<sup>a</sup> and Marco A. Z. Ayub<sup>\*,a</sup>

<sup>a</sup>Grupo de Biotecnologia, Bioprocessos e Biocatálise, Instituto de Ciência e Tecnologia de Alimentos and

<sup>b</sup>Laboratório de Sólidos e Superfícies, Instituto de Química,

Universidade Federal do Rio Grande do Sul (UFRGS), 91501-970 Porto Alegre-RS, Brazil

We carried out the physico-chemical characterization of Immobead 150, a hydrophobic support for the immobilization of lipases. *Thermomyces lanuginosus* lipase (TLL) was immobilized on Immobead 150 by multipoint covalent attachment (ImmTLL) and the morphological, textural, structural, thermal, and physico-chemical properties of the support, before and after enzyme immobilization, were investigated. Immobead 150 presents approximately 1,000  $\mu\text{mol}$  of epoxy groups *per* gram of support, a high hydrophobicity, and good thermal stability. The spherical particles of Immobead 150 present average diameters of 155  $\mu\text{m}$ , specific surface areas of 137  $\text{m}^2 \text{g}^{-1}$  and pore volumes of 0.37  $\text{cm}^3 \text{g}^{-1}$ , showing pores in the region of the micro and meso sizes. The immobilization process of TLL (150  $\text{mg g}^{-1}$ ) caused a decrease of the specific area and pore volumes, to 63  $\text{m}^2 \text{g}^{-1}$  and 0.25  $\text{cm}^3 \text{g}^{-1}$ , respectively, as a result of coating of the support surface by the enzyme molecule. However, the immobilization process did not affect the morphology of the support. The obtained biocatalyst was effective for the syntheses of fatty acid ethyl esters (biodiesel), and of aroma esters, showing yields of 68 and 70%, respectively, similar to commercial preparations used as controls.

**Keywords:** Immobead 150, support characterization, lipase immobilization, butyl butyrate, fatty acid ethyl esters

### Introduction

Enzyme immobilization on solid supports is useful to produce biocatalysis for many fields of applications, such as biotransformations, organic chemistry, and biomedicine.<sup>1,2</sup> One of the most important aspects for the development of different supports for enzyme immobilization is their possible reuse in repeated batch cycles or in continuous process.<sup>3</sup> Supports must present sufficient amount of functional groups on their surfaces, allowing interaction with enzyme molecules. Furthermore, supports should have mechanical and morphological properties that allow their use under industrial conditions, where shear force and temperature stresses are often present. Important aspects that need to be considered, usually interrelated, are the physico-chemical characteristics of the support (available chemical groups, hydrophobicity), and its structural characteristics, such as specific surface area and pore volume and size.<sup>4-6</sup>

Concerning the enzyme to be immobilized, the size of the molecule and the concentration of the protein supplied are of great importance for the immobilization protocol. Therefore, properties of immobilized preparations are dependent on both the properties of the enzyme and the support material. The interaction between them provides an immobilized enzyme system showing specific chemical, biochemical, mechanical, and kinetic properties.<sup>7,8</sup>

A variety of matrices have been used as support materials for enzyme immobilization.<sup>3,9-12</sup> Any solid material that contains cavities, channels, or interstices may be regarded as porous, which is a property of major importance for the practical applications of support materials.<sup>13</sup> According to IUPAC recommendations,<sup>13</sup> pores with free diameters smaller than 2 nm are classified as micropores, those in the range of 2 to 50 nm are mesopores, and those larger than 50 nm, macropores. The pore size characterization is important because enzyme molecules having sizes equal to or larger than that of the support pore will produce low immobilization loadings and will simply

\*e-mail: mazayub@ufrgs.br

adsorb on the external surface, creating a poorly operational biocatalyst. In contrast, small molecule enzymes, much smaller than the support porosity, will freely penetrate the pore support.<sup>14</sup> Bosley and Clayton<sup>15</sup> studied the adsorption of *Mucor miehei* lipase (approximately 5 nm) on controlled-pore glass of eight different pore sizes, functionalized with methyl groups. According to these authors, the pore diameter should be about 5-fold the protein diameter in order to prevent restrictions to the access of the enzyme. However, the immobilization efficiency is independent of pore diameter only for pore sizes bigger than 100 nm.<sup>15</sup>

Another important property of immobilization supports is their hydrophobicity. Supports with more hydrophobic surfaces are very interesting for lipase immobilization because they facilitate enzyme activation on their hydrophobic interfaces directing the enzyme approximation to support during the immobilization process.<sup>12</sup> Therefore, lipases recognize the hydrophobicity of the support in a similar way as they do in relation to their natural substrates, fatty acids.<sup>4,12</sup>

Supports containing epoxy groups on their surface are among the most widely used for lipase immobilization because these chemical groups are short spacer arms and can react with many nucleophilic groups present on the protein surface (e.g., Lys, Cys, His, Tyr), and, in less extension, with carboxylic groups. Concerning the lipase from *Thermomyces lanuginosus*, which has only seven Lys groups in its surface, this intense multipoint covalent attachment would be difficult to be achieved. The most adequate methods for multipoint covalent attachment involve epoxy or glyoxyl supports.<sup>16</sup> In addition, epoxy groups are very stable, making possible to perform long-term incubations of enzyme molecules under alkaline conditions in order to get a multipoint covalent attachment (e.g., involving a number of Lys residues with a relatively high pK value).<sup>17</sup> Covalent attachment is common for high surface area support matrices with large pore diameters, where substrate and product can freely diffuse without enzyme leaching. Unfortunately, the covalent attachment of enzymes to support generally reduces the activity of the enzyme. While these immobilization strategies have their distinct advantages and disadvantages, they can be combined or modified to overcome their limitations to various degrees.<sup>14</sup>

The most common synthetic polymers used as support for enzyme immobilization are represented by acrylic resins, such as Eupergit®-C.<sup>7</sup> They are macroporous copolymers of *N,N'*-methylene-bi-(methacrylamide), glycidyl methacrylate, allyl glycidyl ether, and methacrylamide, showing average particle sizes around 170 nm and pore diameters of about 20-30 nm. These supports are hydrophilic and stable, both

chemically and mechanically, over a large range of pH, and do not swell or shrink even upon exposure to drastic pH changes.<sup>7</sup> On the other hand, Immobead 150 is a commercial support of methacrylate copolymers with epoxy functions, having an average particle size of 150-300 µm. Although some commercial enzymatic derivatives of this product are available, there are few reports dealing with the enzyme immobilization using this support. Immobead 150 has shown interesting characteristics such as the presence of epoxy groups and the stability of the immobilized enzyme when operated in a continuous-flow reactor.<sup>18</sup> However, the morphological, textural, and physico-chemical characteristics of Immobead 150 and the biocatalyst system are not known. It has also been shown that the nature (internal morphology, hydrophobicity of the surface, etc.) of the support may importantly affect the final properties of the immobilized enzyme, such as its activity, stability, selectivity, and specificity.<sup>12</sup> Therefore, more studies are needed to determine the characteristics and possible applications for this support.

In the light of these considerations, the main objective of this study was to investigate the morphological, textural, and physico-chemical characteristics of Immobead 150 before and after immobilization. We produced a biocatalyst, where lipase from *Thermomyces lanuginosus* (TLL) was covalently immobilized on Immobead 150 mediated by the reaction between the surface epoxy groups on the support and Lys groups on the enzyme molecule. In addition, the obtained derivative biocatalyst was applied in two different reaction systems, for the synthesis of fatty acid ethyl esters (biodiesel) and aroma esters production.

## Experimental

### Materials

Lipase from *T. lanuginosus* (TLL, Lipolase 100 L, soluble form) and TLL immobilized on a silicate support (Lipozyme TL-IM) were kindly provided by Novozymes (Spain). Immobead 150, commercial derivative of TLL immobilized on Immobead 150 (ImmTLLc), *p*-nitrophenyl palmitate (*p*NPP), *p*-nitrophenol (*p*NP), and Rose Bengal were purchased from Sigma-Aldrich Co. (St. Louis, USA). All other reagents used were of analytical grade.

### Hydrolytic activity of lipase

The hydrolysis reaction was carried out using *p*NPP. Substrate solution was prepared mixing one volume of 10 mM solution of *p*NPP in 2-propanol with nine volumes of 10 mM phosphate buffer solution pH 8.0 containing

0.44% (mass fraction) Triton X-100 and 0.11% (mass fraction) Arabic gum. The lipase activity was measured using 100  $\mu\text{L}$  of lipase solution or suspension and 900  $\mu\text{L}$  of the substrate solution (10 mM *p*NPP) at 55 °C for 2 min. The absorbance of *p*-nitrophenol released was spectrophotometrically monitored at 410 nm. One unit of lipase activity was expressed as the release of 1  $\mu\text{mol}$  *p*-nitrophenol *per* minute under the assay conditions. The calibration curve was prepared using *p*-nitrophenol as standard. Values are given as mean  $\pm$  standard deviation in triplicate for each point.

#### Protein determination

Soluble protein was determined by the Bradford method<sup>19</sup> using bovine serum albumin (BSA) as protein standard.

#### Immobilization multipoint on Immobead 150 with different ionic strengths

1 g of support was resuspended in 10 mL of enzyme solution in different molarities of sodium carbonate buffer pH 10.5 (0.01, 0.05, 0.1, 0.5, and 1 M) at 24 °C for 24 h, under gentle agitation on a roller mix, for multipoint attachment. The amino groups present in the lysine residues on the enzyme external surface are very reactive when unprotonated. This reactivity causes a multiinteraction with the groups of the support.<sup>20</sup> After immobilization, successive washings with buffer were done to remove the excess of enzyme until no activity was detected in the washed fractions. To check the covalent binding, washings with NaCl (1 M) and ethylene glycol (30% volume fraction) were performed to eliminate ionic and hydrophobic interactions between enzyme and support, leaving only the covalently immobilized enzymes.

Immobilization efficiency and yields were followed by measuring the hydrolytic activities and the protein concentration in the supernatant solution for all experiments. Immobilization yield was calculated after determining the amount of enzyme units (equation 1) that disappeared from the supernatant and comparing with the initial enzyme concentrations offered to reaction. Immobilization efficiency (equation 2) was calculated after determining the activity of the immobilized enzyme and comparing with total residual enzyme activity that remains in the enzyme solution after immobilization and by subtracting this activity from the total starting activity.<sup>21</sup>

$$\text{Immobilization yield} = \frac{(\text{total starting activity} - \text{total residual activity})}{\text{total starting activity}} \times 100 \quad (1)$$

$$\text{Efficiency} = \frac{\text{observed activity}}{(\text{total starting activity} - \text{total residual activity})} \times 100 \quad (2)$$

#### Immobilization with different loads of TLL

The concentration protein *per* gram of support varied from 10 to 150 mg  $\text{g}^{-1}$ . 1 g of support was resuspended in 10 mL of enzyme solution in sodium phosphate buffer pH 10.5 (10 mM). After the immobilization process, the preparations were submitted to the same successive washings as described above.

#### Morphological and textural characterization

Images of the support were obtained by scanning electron microscopy (SEM; JEOL, model JSM 6060, Japan) operating at 10 kV. The size distribution was determined using the Quantikov software from the original image containing 294 particles. Textural characteristics of the samples were evaluated by  $\text{N}_2$  adsorption-desorption isotherms at 77 K, using the Tristar II Krypton 3020 Micromeritics equipment. Samples were degassed at 40 and 120 °C under vacuum, for 48 and 10 h, respectively. The specific surface areas and pore volume were determined by using the BET (Brunauer-Emmett-Teller) method,<sup>22</sup> whereas the pore size distribution was estimated using the BJH (Barrett-Joyner-Halenda) and DFT (density functional theory) methods.<sup>22,23</sup>

#### Thermal properties

The thermogravimetric analysis (TGA) was performed using the Shimadzu thermal analyzer Model TA50, from 20 up to 600 °C under argon atmosphere, at a heating rate of 10 °C  $\text{min}^{-1}$ .

#### Structural characterization

Changes on the molecular structure of Immobead 150 and ImmTLL were determined by Fourier transform infrared (FTIR) spectroscopy with a Varian 640-IR spectrometer. Samples were analyzed using the ATR (attenuated total reflectance) technique. The spectra were obtained at room temperature (25 °C) with 40 cumulative scans and 4  $\text{cm}^{-1}$  of resolution.

#### Hydrophobicity of the supports

The surface hydrophobicity of the support was estimated by determining the amount of hydrophobic dye Rose Bengal that was adsorbed on it.<sup>24,25</sup> To determine the hydrophobicity, a fixed amount of support (0.1 g) was mixed with 10 mL

Rose Bengal solution ( $20 \mu\text{g mL}^{-1}$ ), and kept under gentle agitation for 3 h. The amount of Rose Bengal adsorbed was then determined by absorbance ( $\lambda_{\text{max}} = 548 \text{ nm}$ ) of the solution after separating it from the support. The adsorption of the dye was expressed as the relation between the adsorbed dye concentration and the mass of support used.

#### Determination of epoxy groups

Epoxy groups (oxirane) in the supports were determined according to the methodology described by Sundberg and Porath,<sup>26</sup> with small modifications. Support (0.1 g) was added to 10 mL of 1.3 M sodium thiosulfate solution pH 7.0 and the epoxy content was determined by titration using 0.1 M hydrochloric acid. The amount of epoxy groups was calculated using the amount of HCl that was required to maintain the neutrality of the suspension.

#### Reaction of esterification and analysis

Esterification reactions were carried out in 50 mL Erlenmeyer flask using *n*-hexane as organic solvent. Butyl butyrate was prepared by mixing 0.3 M *n*-butanol and 0.1 M butyric acid, followed by the addition of the immobilized lipase (40% by substrate weight). The mixtures were incubated at  $37 \text{ }^\circ\text{C}$  and 100 rpm for 4 h.

The progress of esterification was monitored by titration determining the residual acid content. Samples were withdrawn (0.5 mL) and diluted in 5 mL of ethanol as quenching agent, and titrated with 0.005 N NaOH using phenolphthalein as the end-point indicator. The amount of ester was calculated as being equivalent to the acid consumed.

#### Reaction of transesterification and analysis

In Erlenmeyer flasks, 1 g of soybean oil was mixed with ethanol (6:1 alcohol:soybean oil molar ratio) and 15% of immobilized lipase, based on oil weight. The reactions were carried out in an orbital shaker at 100 rpm,  $37 \text{ }^\circ\text{C}$  for 4 h. After reaction completion, 2 mL of distilled water was added, followed by centrifugation ( $5000 \times g$ , 5 min). The upper phase, containing esters, was analyzed by gas chromatography (Shimadzu, model GC-17A) equipped with a flame ionization detector (FID) and DB5 capillary column (30 m  $\times$  0.25 mm i.d.  $\times$  0.25  $\mu\text{m}$ ) (J&W Scientific). After samples were accurately weighted, an internal standard stock solution (methyl heptadecanoate in heptane) was added to the sample. The amount of sample injected was 1  $\mu\text{L}$ . The chromatographic conditions were: initial column temperature of  $50 \text{ }^\circ\text{C}$ , heating rate of  $10 \text{ }^\circ\text{C min}^{-1}$

until reaching a final temperature of  $310 \text{ }^\circ\text{C}$ . The injector temperature was  $300 \text{ }^\circ\text{C}$ , split ratio 1:30 and the FID detector temperature was  $310 \text{ }^\circ\text{C}$ . The carrier gas used was nitrogen at a flow of  $1.0 \text{ mL min}^{-1}$ . A standard FAEE (fatty acid ethyl esters) mix (C4-C24) from Supelco was used to identify the peaks at different retention times and to correct the peak area using the response factors of the compound. The FAEE content was calculated using the compensated normalization method with internal standardization, based on the European standard DIN EN 14103.<sup>27</sup>

## Results and Discussion

#### Multipoint Immobilization of TLL on Immobead 150 using different ionic strengths and different loads of enzyme

The influences of the molarity of buffer on the immobilization yield and the efficiency of TLL preparations using  $20 \text{ mg g}^{-1}$  of protein on Immobead 150 are presented in Figure 1. The increase in molarity caused a gradual decrease in immobilization efficiency. Therefore, the 10 mM buffer produced the best results in terms of efficiency, without causing any losses in yields of immobilization. According to Barbosa *et al.*,<sup>28</sup> lipases are expected to be immobilized in low ionic strength environments involving the hydrophobic areas surrounding their active sites, which would allow the interfacial activation of the molecule. Moreover, at low ionic strengths, there is a reduction of lipase aggregation caused by reduced hydrophobic interactions, which allows better efficiency after immobilization.

The influence of the amount of protein loading on the yield and the efficiency of TLL preparations are

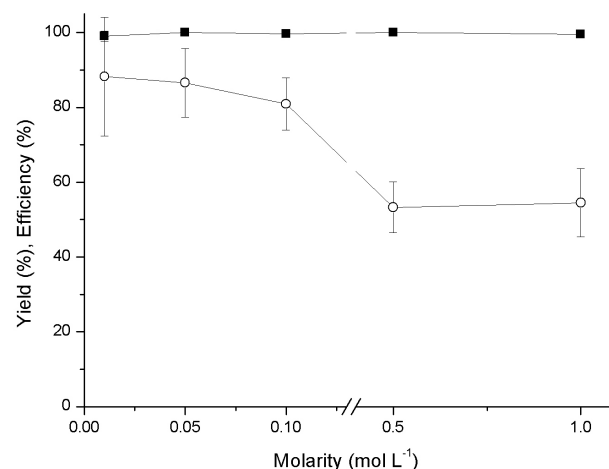


**Figure 1.** Variations of molarity of the immobilization buffer. Conditions: Immobead 150 and protein load of  $20 \text{ mg g}^{-1}$  of TLL, sodium phosphate buffer pH 10.5 at  $24 \text{ }^\circ\text{C}$  for 24 h (ImmTLL). Results are expressed in terms of percentages of yield (■), and efficiency (○). The results are the mean of triplicates.

shown in Figure 2. The results indicate that the highest immobilization yield and efficiency were observed using low protein concentrations, but the efficiencies ( $76 \pm 4\%$ ) remained high up to a load of 150 mg protein. These results correlates well with previous reports on the literature,<sup>29</sup> in which, using the same protocol but 1 M immobilization buffer and protein loads varying from 5 to 20 mg g<sup>-1</sup>, it was observed a decrease in the efficiency inversely proportional to protein load. This loss of efficiency can be attributed to high ionic strength of the immobilization buffer, possibly causing the aggregation of the protein.

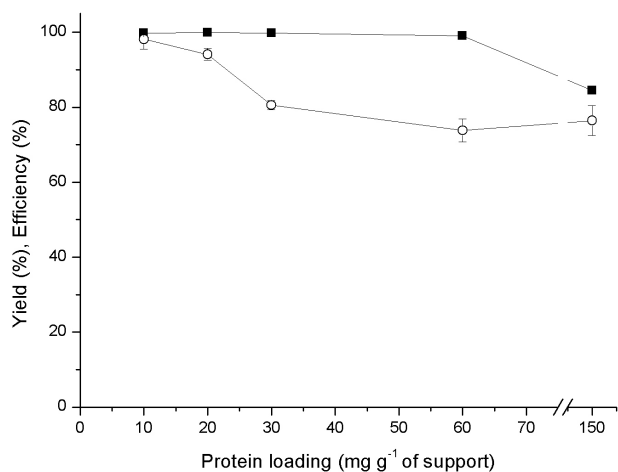


**Figure 2.** Effect of protein loading on ImmTLL. Results are expressed in terms of percentages of yield (■), and efficiency (○). The results are the mean of triplicates.

Therefore, the enzyme load of 150 mg enzyme *per* gram of support was selected for further experiments because of the higher activity of the immobilized derivative obtained by this condition.

#### Morphological and textural characterization

The SEM analysis highlights the morphology of Immobead 150 before and after immobilization (Figures 3A and 3B, respectively), showing that Immobead 150 has spherical form and presents a scattered variation in particle sizes. The size distribution histogram is depicted in Figure 3C. The average estimated diameter was 155 μm, with a standard deviation of 37 μm, for Immobead 150 with or without enzyme. The morphology of the support was not changed either before or after the immobilization at the observed level.

The N<sub>2</sub> adsorption-desorption isotherms of Immobead 150 are shown in Figure 4A. The isotherms are of type-IV,<sup>22</sup> which corresponds to a mesoporous material. The immobilization process affected the

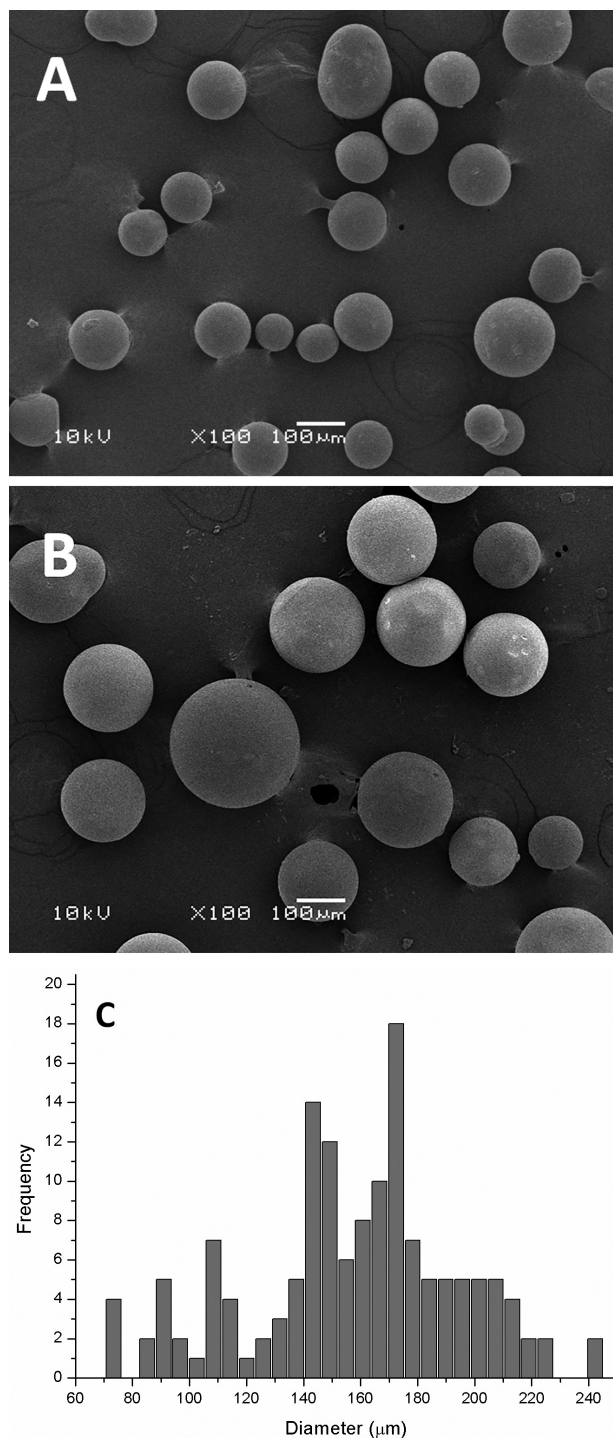


**Figure 3.** Morphological characterization of supports. Scanning electron micrograph (10 kV; 100×): (A) Immobead 150; (B) ImmTLL; (C) size distribution of Immobead 150.

specific surface area, which decreased from  $137 \pm 5$  to  $63 \pm 5$  m<sup>2</sup> g<sup>-1</sup>. Although the adsorbed gases in the support were removed before analysis by degassing at 40 and 120 °C, the specific surface area results did not show differences between the samples at different temperatures of degassing. Sharma *et al.*<sup>30</sup> investigated the specific area

of Immobead 150 and Immobead 150-*Candida antarctica* B lipase using degassing at 60 °C for 1 h, where they showed a surface area of around 218 and 118 m<sup>2</sup> g<sup>-1</sup>, respectively. The differences between the results of their work and the values obtained by us suggest a non-uniformity of this commercial support.

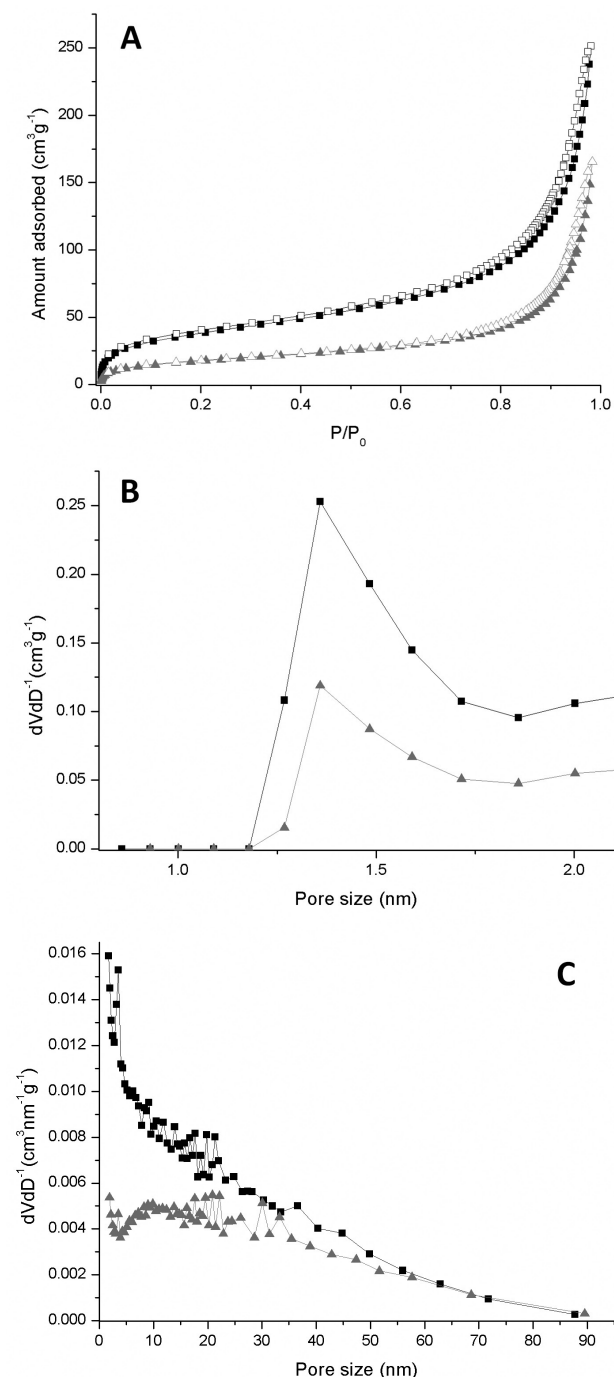


**Figure 4.** Textural characterization of supports: (A) N<sub>2</sub> adsorption (■,▲) and desorption (□,△) isotherms; (B) DFT micropore size distribution; (C) BJH pore size distribution; (■ and black line) represents the support Immobead 150 before immobilization; (▲ and gray line) represents the derivative (ImmTLL).

The micropore size distribution curves (Figure 4B), calculated by DFT method, shows that the support has micropores in the region between 1.2 and 2 nm. The micropore size distribution curve shows a similar profile in the derivative after immobilization, but the quantity of micropores was reduced after the immobilization process. Moreover, this support is a slightly mesoporous material, as shown by the BJH curves, presenting cumulative pore volume of 0.37 ± 0.01 cm<sup>3</sup> g<sup>-1</sup> before immobilization and 0.25 ± 0.01 cm<sup>3</sup> g<sup>-1</sup> after immobilization. Comparatively, silica MS-3030 presents a mean pore volume of 2.9 cm<sup>3</sup> g<sup>-1</sup>,<sup>31</sup> polypropylene powder Accurel MP 1000 of 1.9 cm<sup>3</sup> g<sup>-1</sup>,<sup>32</sup> and macroporous polypropylene Accurel MP1004 of 2 cm<sup>3</sup> g<sup>-1</sup>,<sup>33</sup> both having higher porosities than Immobead 150. On the other hand, meso-structured onion-like silica presents a pore volume of 0.2 cm<sup>3</sup> g<sup>-1</sup> and chitosan macroparticles only 0.1 cm<sup>3</sup> g<sup>-1</sup>,<sup>11,34</sup> very low porosities when compared to Immobead 150.

Diffusional restrictions of substrate may be influenced by particle size and pore diameter.<sup>35,36</sup> A disordered network of pores and channels would only allow the smallest substrates to penetrate the biocatalyst, whereas bigger substrates would obstruct the channels, slowing down the reactions. Thus, a heterogeneous pore size distribution interferes not only with the enzyme load on the internal surfaces, but also with the diffusion of substrates and/or products.<sup>31</sup> Immobead 150 did not show a unique pore profile (Figure 4C), presenting pores throughout the mesoporous region, being more prominent the pores of smaller size. Thus, observing the textural data from the support before and after immobilization we can say that the most affected pores are those smaller than 20 nm, thus the enzyme should be immobilized preferably blocking the smaller pores of the support.

Serra *et al.*<sup>35</sup> investigated the immobilization of lipase from *Candida antarctica* B in mesoporous materials having different pore sizes. They found that, during the adsorption process, diffusion limitations occurred when the pore size was similar to the enzyme size, but these drawbacks disappeared when the pore diameter was around twice as large as the enzyme molecule dimension.<sup>35</sup> According to the protein structure explorer (PDB, 1dt5),<sup>37</sup> the size of the *T. lanuginosus* lipase molecule is around 5 nm, and this molecular size can drastically reduce pore volume when the enzyme penetrates it, or even totally block the micropore and part of mesopore area. Therefore, comparing data from the literature with our results, we can suggest that increasing enzyme load will induce a large amount of enzyme to penetrate the pores of the support, thus blocking them, causing a reduced efficiency of immobilization as shown in Figure 2.

## Thermal properties

The TGA analysis of the support, depicted in Figure 5A, showed that the particles were thermally stable at least up to 200 °C, which is much higher than the temperature used for most of enzymatic reactions. The weight loss of particles between 200 and 450 °C is related to the polymer (Immobead 150) decomposition.

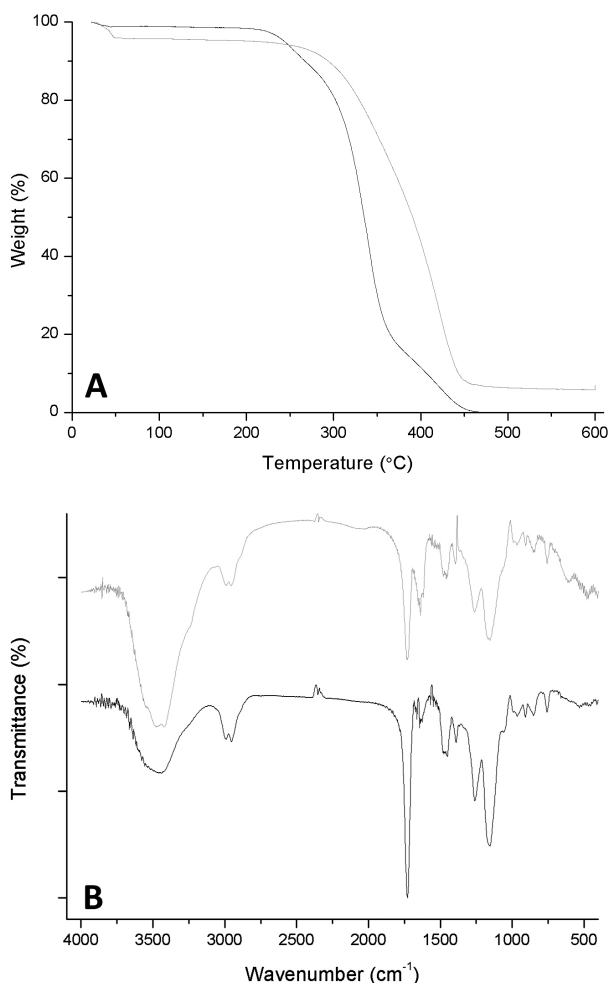


**Figure 5.** TGA curves (Figure A) and FTIR spectra (Figure B) of Immobead 150 (black line), and ImmTLL (gray line).

It was observed a loss of weight around 5% between 20 and 150 °C, probably caused by the water desorption from samples. The fact that this support has a small associated amount of water is remarkable in the sense that enzyme stability can be greatly enhanced when exposed to organic solvents and ionic liquids, as it was observed in a previous work.<sup>29</sup> The control of water content on enzymatic synthesis reactions is important because this fact can affect the reaction either positively or negatively. Water acts as a ‘lubricant’, maintaining the enzyme in the active conformation. On the other hand, water can also promote

the hydrolysis of the substrate, thus decreasing the yield of products.<sup>18,38</sup> These effects are dependent on the amount of water present in the reaction, as it has been demonstrated by Rodrigues *et al.*,<sup>38</sup> who showed that a small amount of water (6.5% by weight of oil) presented a positive effect in the biodiesel synthesis.

## Structural characterization

FTIR spectra of Immobead 150 and ImmTLL are presented in Figure 5B. The broad band between 3,100 and 3,700 cm<sup>-1</sup> is attributed to the O–H stretching vibration, mainly from water, which overlaps the amine stretching vibrations (N–H) in the same region. The bands between 2,800 and 3,000 cm<sup>-1</sup> are attributed to the C–H stretching vibration,<sup>39</sup> whereas the strong sharp peak at 1,700 cm<sup>-1</sup> corresponds to carbonyl group of the carboxylic acid functional group.<sup>30</sup> The peak at 1,500 cm<sup>-1</sup> is for the bending vibration of free amine present in the enzyme and peaks ranging from 1,200 to 600 cm<sup>-1</sup> indicate the finger print region and are characteristic of Immobead 150.<sup>30</sup>

## Determination of epoxy groups

The Immobead 150 presented about 1,000 μmol epoxy groups *per* gram of support. Bezbradica *et al.*<sup>40</sup> studied other commercial epoxy supports, Eupergit® and Eupergit C 250L, which presented around 600 and 250 μmol g<sup>-1</sup>, respectively. We can observe in Figure 6 that the immobilization of 150 mg g<sup>-1</sup> of TLL in Immobead 150 (ImmTLL) reduced about 50% of the available epoxy groups. Concerning the use of glycine, the reagent was capable of blocking the epoxy groups, thus the support presented properties similar to those of the commercial control (ImmTLLc).<sup>41</sup>

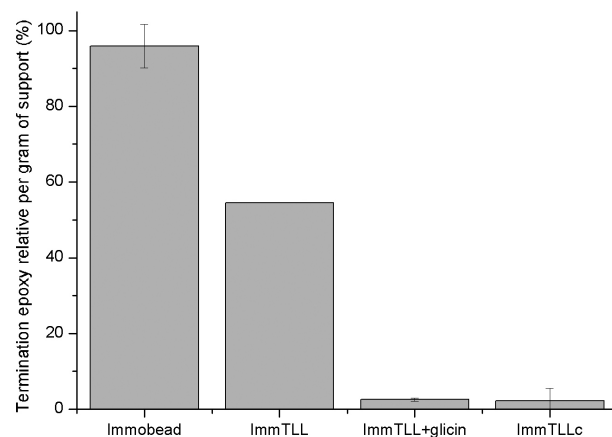


**Figure 6.** Relative comparison of the number of epoxy groups on the surface of Immobead 150. Results are the mean of triplicates.

### Hydrophobicity of the supports

The immobilization caused only a small decrease in the original hydrophobicity of the support, differently from the commercial derivative of Immobead 150 (ImmTLLc), which presented a reduction in hydrophobicity of almost eight times (Figure 7). We also compared the hydrophobicity with other commercial supports widely studied for the immobilization of lipases, such as Octyl Sepharose and styrene-divinylbenzene beads (MCI GEL CHP 20P, Supelco). Compared to them, the Immobead 150 presented the highest hydrophobicity.

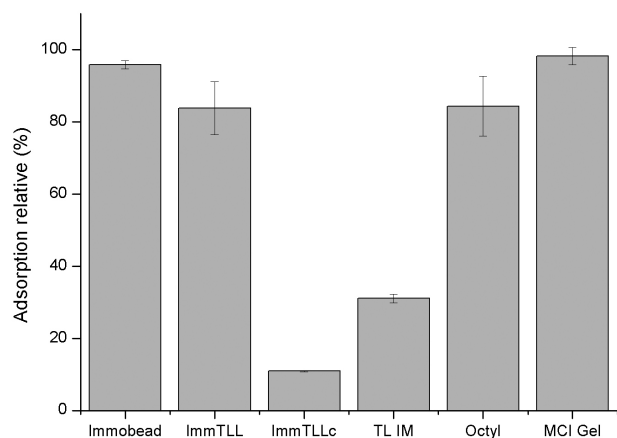


**Figure 7.** Relative adsorption of hydrophobic marker Rose Bengal by supports. Results are the mean of triplicates.

The effects caused by the hydrophobicity of supports on the activity recovery, after immobilization, of different enzymes vary considerably. Enzymes such as  $\beta$ -galactosidase from *A. oryzae* and epoxide hydrolase from *A. niger*, when immobilized on hydrophobic epoxy supports, were fully inactivated or retained only 30% of their activities, respectively.<sup>17</sup>

Although high hydrophobicity of the support generally enhances activity recovery in the immobilization process of lipases, it presented a problem in the case of meso- and macroporous supports. This is because the buffered aqueous solution containing the enzyme should reach the whole surface of the support, both the external as well as the inner surface of the pore channels. The access to the internal structure can be limited by the wettability of the support, thus for very hydrophobic surfaces the aqueous phase could not diffuse into the pores, reaching only the external part of the channel.<sup>5</sup> Thus, this property has a significant influence on the distribution of enzyme molecules in the support. In this case, the biocatalyst particle would only contain enzyme molecules in the outside surface, whereas the inner channels would remain empty, as confirmed by results of morphological and textural characterization.

### Reactions of esterification and transesterification

In order to test the biocatalyst prepared in this work, we applied the immobilized lipase in Immobead 150 for the synthesis of aroma esters and fatty acid ethyl esters (biodiesel), and compared the results for commercial enzymes (Figures 8A and 8B). The synthesis of aroma esters such as butyl butyrate (pineapple flavor) was chosen as a study model because of its importance in the food industry.

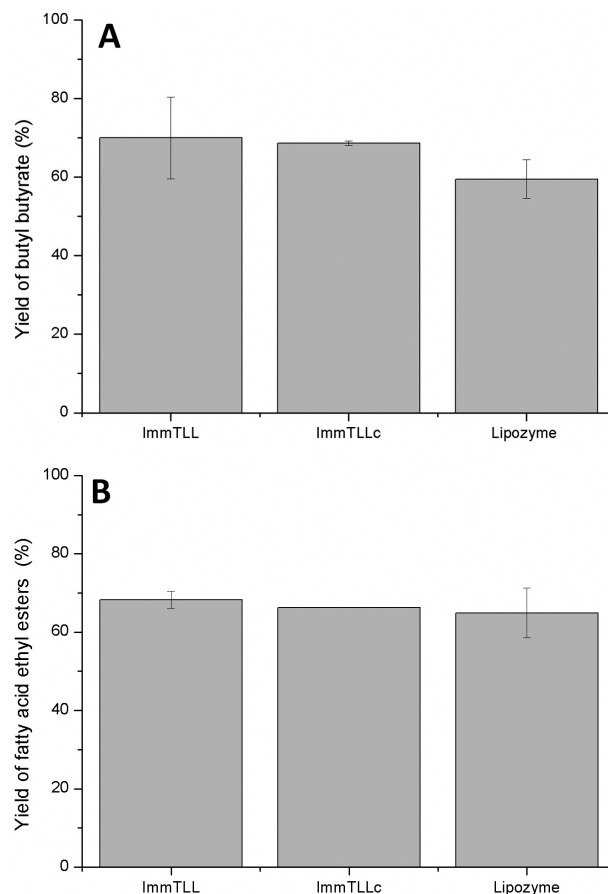


**Figure 8.** Butyl butyrate synthesis and fatty acid ethyl esters synthesis. Controls: commercial TLL immobilized in supports Immobead 150 and Lipozyme TL IM. Results are the mean of duplicates.

ImmTLL was compared with the commercial TLL preparations as Lipozyme TL-IM and commercial derivative of Immobead 150 (ImmTLLc) for the synthesis of butyl butyrate (Figure 8A) and fatty acid ethyl esters (Figure 8B). Results show that all preparations presented similar performances, producing approximately 70% yield of synthesis in the short reaction time of 4 h. Under optimized conditions, the commercial Lipozyme TL-IM and the MCI Gel CHP20P support immobilized with 120 mg g<sup>-1</sup> of TLL, showed yields around 60 and 80% of butyl butyrate after 4 h, respectively.<sup>42</sup> Commercial

Lipozyme TL-IM derivative showed lower than 20% fatty acid ethyl esters yields when used with olive and palm oil.<sup>43</sup> These results demonstrate the potential applicability of the support Immobead 150 with TLL immobilized via multipoint attachment for esterification and transesterification reactions.

When applied for butyl butyrate synthesis, ImmTLL has shown a high operational stability after 30 days of continuous operation on a packed-bed reactor, with higher than 60% of the initial activity at the end of the run.<sup>44</sup> This is one of the most interesting possibilities of using a continuous system to obtain ester in an industrial scale.

One of the main problems that should be solved to improve the enzymatic synthesis of biodiesel is the regiospecificity of enzymes, and it would be important to obtain reaction yields close to 100% in order to make the enzymatic process competitive against the chemical process. The TLL biocatalyst possess an sn-1,3 regiospecificity and the acyl migration from sn-2 position to sn-1,3 position should occur during the reaction. In fact, this migration occurs spontaneously during the reaction. In the literature different factors are cited as influencing the acyl migration. The properties of the support, temperature and solvent of the reaction were the most significant parameters to control the acyl migration.<sup>16</sup> These parameters will be studied in the future by this research group in a continuous process of reactions by fatty acid ethyl esters synthesis.

## Conclusions

The immobilization technique is a method that allows the reuse and facilitates the recovery of the biocatalyst and products. Immobilization depends upon the choice of the enzyme and support, and the methods used for the immobilization itself. It is, therefore, of fundamental importance to understand the characteristics of the support in order to develop appropriate immobilization techniques. The morphological and physico-chemical characteristics of Immobead 150 were studied using different techniques. The spherical particles of Immobead 150 presented wide pore size range, showing pores in the region of micro and mesopores. The Immobead 150 support appears to be very interesting for the immobilization of lipases, especially because of its epoxy groups, high hydrophobicity, and thermal stability. Using multipoint attachment through external Lys residues of TLL and epoxy groups of Immobead 150, we produced a biocatalyst possessing similar properties of commercial derivatives concerning the synthesis of aromas and fatty acid ethyl esters.

## Supplementary Information

Supplementary data (Figure S1, immobilization buffer effect on enzyme aggregation) are available free of charge at <http://jbcs.sbq.org.br> as PDF file.

## Acknowledgments

This work was partially supported by grants from the Conselho Nacional de Desenvolvimento Científico e Tecnológico (CNPq, Brazil) and Fundação de Amparo à Pesquisa do Estado do Rio Grande do Sul (FAPERGS, RS). We also would like to thank the Centro de Microscopia e Microanálise (CMM, UFRGS) for their support on the microscopy analysis. The first author acknowledges the scholarship from CNPq.

## References

1. Poppe, J. K.; Matte, C. R.; Peralba, M. C. R.; Fernandez-Lafuente, R.; Rodrigues, R. C.; Ayub, M. A. Z.; *Appl. Catal., A* **2015**, *490*, 50.
2. de Abreu, L.; Fernandez-Lafuente, R.; Rodrigues, R. C.; Volpato, G.; Ayub, M. A. Z.; *J. Mol. Catal. B: Enzym.* **2014**, *99*, 51.
3. Mihailović, M.; Stojanović, M.; Banjanac, K.; Carević, M.; Prlainović, N.; Milosavić, N.; Bezbradica, D.; *Process Biochem.* **2014**, *49*, 637.
4. Galarneau, A.; Mureseanu, M.; Atger, S.; Renard G.; Fajula, F.; *New J. Chem.* **2006**, *30*, 562.
5. Blanco, R. M.; Terreros, P.; Muñoz, N.; Serra, E.; *J. Mol. Catal. B: Enzym.* **2007**, *47*, 13.
6. Hartmann, M.; Kostrov, X.; *Chem. Soc. Rev.* **2013**, *42*, 6277.
7. Homaei, A.; Sariri, R.; Vianello, F.; Stevanato, R.; *J. Chem. Biol.* **2013**, *6*, 185.
8. Zhou, Z.; Hartmann, M.; *Top. Catal.* **2012**, *55*, 1081.
9. Mendes, A.; de Castro, H.; Rodrigues, D. S.; Adriano, W.; Tardioli, P.; Mammarella, E.; Giordano, R. C.; Giordano, R. L. C.; *J. Ind. Microbiol. Biotechnol.* **2011**, *38*, 1055.
10. Silva, W. S. D.; Lapis, A. A. M.; Suarez, P. A. Z.; Neto, B. A. D.; *J. Mol. Catal. B: Enzym.* **2011**, *68*, 98.
11. Klein, M. P.; Nunes, M. R.; Rodrigues, R. C.; Benvenuti, E. V.; Costa, T. M. H.; Hertz, P. F.; Ninow, J. L.; *Biomacromolecules* **2012**, *13*, 2456.
12. Garcia-Galan, C.; Barbosa, O.; Hernandez, K.; Santos, J.; Rodrigues, R.; Fernandez-Lafuente, R.; *Molecules* **2014**, *19*, 7629.
13. Rouquerol, J.; Avnir, D.; Fairbridge, C. W.; Everett, D. H.; Haynes, J. H.; Pernicone, N.; Ramsay, J. D. F.; Sing, K. S. W.; Unger, K. K.; *Pure Appl. Chem.* **1994**, *66*, 1739.
14. Tran, D. N.; Balkus, K. J.; *ACS Catal.* **2011**, *1*, 956.

15. Bosley, J. A.; Clayton, J. C.; *Biotechnol. Bioeng.* **1994**, *43*, 934.
16. Fernandez-Lafuente, R.; *J. Mol. Catal. B: Enzym.* **2010**, *62*, 197.
17. Mateo, C.; Grazu, V.; Palomo, J. M.; Lopez-Gallego, F.; Fernandez-Lafuente, R.; Guisan, J. M.; *Nat. Protoc.* **2007**, *2*, 1022.
18. Babich, L.; Hartog, A. F.; Van der Horst, M. A.; Wever, R.; *Chem. Eur. J.* **2012**, *18*, 6604.
19. Bradford, M. M.; *Anal. Biochem.* **1976**, *72*, 248.
20. Rodrigues, R. C.; Godoy, C. A.; Volpato, G.; Ayub, M. A. Z.; Fernandez-Lafuente, R.; Guisán, J. M.; *Process Biochem.* **2009**, *44*, 963.
21. Sheldon, R. A.; van Pelt, S.; *Chem. Soc. Rev.* **2013**, *42*, 6223.
22. Gregg, S. J.; Sing, K. S. W.; *Adsorption, Surface Area and Porosity*, 2<sup>nd</sup> ed; Academic Press: London, UK, 1982.
23. Lastoskie, C.; Gubbins, K. E.; Quirke, N.; *J. Phys. Chem.* **1993**, *97*, 4786.
24. Doktorovova, S.; Shegokar, R.; Martins-Lopes, P.; Silva, A. M.; Lopes, C. M.; Müller, R. H.; Souto, E. B.; *Eur. J. Pharm. Sci.* **2012**, *45*, 606.
25. Gupta, K. C.; Jabrail, F. H.; *Carbohydr. Polym.* **2006**, *66*, 43.
26. Sundberg, L.; Porath, J.; *J. Chromatogr. A* **1974**, *90*, 87.
27. EN 14103; *Fat and Oil Derivatives - Fatty Acid Methyl Esters (FAME) - Determination of Esters and Linolenic Acid Methyl Esters Content*; European Committee for Standardization: Brussels, 2001.
28. Barbosa, O.; Ortiz, C.; Torres, R.; Fernandez-Lafuente, R.; *J. Mol. Catal. B: Enzym.* **2011**, *71*, 124.
29. Matte, C. R.; Bussamara, R.; Dupont, J.; Rodrigues, R. C.; Hertz, P. F.; Ayub, M. A. Z.; *Appl. Biochem. Biotechnol.* **2014**, *172*, 2507.
30. Sharma, A.; Chaurasia, S. P.; Dalai, A. K.; *Can. J. Chem. Eng.* **2014**, *92*, 344.
31. Blanco, R. M.; Terreros, P.; Fernández-Pérez, M.; Otero, C.; Díaz-González, G.; *J. Mol. Catal. B: Enzym.* **2004**, *30*, 83.
32. Madalozzo, A. D.; Muniz, L. S.; Baron, A. M.; Piovan, L.; Mitchell, D. A.; Krieger, N.; *Biocatal. Agric. Biotechnol.* **2014**, *3*, 13.
33. Salis, A.; Pinna, M.; Monduzzi, M.; Solinas, V.; *J. Mol. Catal. B: Enzym.* **2008**, *54*, 19.
34. Jun, S. H.; Lee, J.; Kim, B. C.; Lee, J. E.; Joo, J.; Park, H.; Lee, J. H.; Lee, S. M.; Lee, D.; Kim, S.; Koo, Y. M.; Shin, C. H.; Kim, S. W.; Hyeon, T.; Kim, J.; *Chem. Mater.* **2012**, *24*, 924.
35. Serra, E.; Mayoral, Á.; Sakamoto, Y.; Blanco, R. M.; Díaz, I.; *Microporous Mesoporous Mater.* **2008**, *114*, 201.
36. Fernández, O.; Díaz, I.; Torres, C. F.; Tobajas, M.; Tejedor, V.; Blanco, R. M.; *Appl. Catal., A* **2013**, *450*, 204.
37. Brzozowski, A. M.; Savage, H.; Verma, C. S.; Turkenburg, J. P.; Lawson, D. M.; Svendsen, A.; Patkar, S.; *Biochem. J.* **2000**, *39*, 15071.
38. Rodrigues, R. C.; Volpato, G.; Ayub, M. A. Z.; Wada, K.; *J. Chem. Technol. Biotechnol.* **2008**, *83*, 849.
39. Colthup, N. B.; Daly, L. H.; Wiberley, S. E.; *Introduction to Infrared and Raman Spectroscopy*; Academic Press: San Diego, EUA, 1990.
40. Bezbradica, D.; Mijin, D.; Mihailović, M.; Knežević-Jugović, Z.; *J. Chem. Technol. Biotechnol.* **2009**, *84*, 1642.
41. Mateo, C.; Abian, O.; Fernández-Lorente, G.; Pedroche, J.; Fernández-Lafuente, R.; Guisan, J. M.; *Biotechnol. Prog.* **2002**, *18*, 629.
42. Martins, A. B.; Friedrich, J. L. R.; Cavalheiro, J. C.; Garcia-Galan, C.; Barbosa, O.; Ayub, M. A. Z.; Fernandez-Lafuente, R.; Rodrigues, R. C.; *Bioresour. Technol.* **2013**, *134*, 417.
43. Pedersen, A. T.; Nordblad, M.; Nielsen, P. M.; Woodley, J. M.; *J. Mol. Catal. B: Enzym.* **2014**, *105*, 89.
44. Matte, C. R.; Bordinhão, C.; Poppe, J. K.; Rodrigues, R. C.; Hertz, P. F.; Ayub, M. A. Z.; *J. Mol. Catal. B: Enzym.* **2016**, *127*, 67.

Submitted: September 20, 2016

Published online: December 13, 2016

FAPERGS/CAPES has sponsored the publication of this article.